HHS Public Access

Author manuscript

Arthritis Rheumatol. Author manuscript; available in PMC 2016 March 09.

Published in final edited form as:

Arthritis Rheumatol. 2015 May ; 67(5): 1335–1344. doi:10.1002/art.39062.

Endothelin Receptor Blockade Ameliorates Vascular Fragility in Endothelial Cell–Specific Fli-1–Knockout Mice by Increasing Fli-1 DNA Binding Ability

Kaname Akamata, MD, PhD[1], **Yoshihide Asano, MD, PhD**[1], **Takashi Yamashita, MD**[1], **Shinji Noda, MD, PhD**[1], **Takashi Taniguchi, MD**[1], **Takehiro Takahashi, MD**[1], **Yohei Ichimura, MD**[1], **Tetsuo Toyama, MD**[1], **Maria Trojanowska, PhD**[2], and **Shinichi Sato, MD, PhD**[1]

[1]University of Tokyo Graduate School of Medicine, Tokyo, Japan

[2]Boston University School of Medicine, Boston, Massachusetts

Abstract

Objective—It is generally accepted that blockade of endothelin receptors has potentially beneficial effects on vasculopathy associated with systemic sclerosis (SSc). The aim of this study was to clarify the molecular mechanism underlying these effects using endothelial cell–specific Fli-1–knockout (Fli-1 ECKO) mice, an animal model of SSc vasculopathy.

Methods—Levels of messenger RNA for target genes and the expression and phosphorylation levels of target proteins were determined in human and murine dermal microvascular endothelial cells by real-time quantitative reverse transcription–polymerase chain reaction and immunoblotting, respectively. The binding of Fli-1 to the target gene promoters was evaluated using chromatin immunoprecipitation. Expression levels of Fli-1 and α-smooth muscle actin in murine skin were evaluated using immunohistochemistry. Vascular structure and permeability were evaluated in mice injected with fluorescein isothiocyanate–dextran and Evans blue dye, respectively.

Results—In human dermal microvascular endothelial cells, endothelin 1 induced phosphorylation of Fli-1 at Thr^{312} through the sequential activation of c-Abl and protein kinase Cδ, leading to a decrease in Fli-1 protein levels as well as a decrease in binding of Fli-1 to the target gene promoters, whereas bosentan treatment reversed those effects. In Fli-1 ECKO mice, 4 weeks of treatment with bosentan increased endothelial Fli-1 expression, resulting in vascular stabilization and the restoration of impaired leaky vessels.

Conclusion—The vascular fragility of Fli-1 ECKO mice was improved by bosentan through the normalization of Fli-1 protein levels and activity in endothelial cells, which may explain, in part,

Address correspondence to Yoshihide Asano, MD, PhD, Department of Dermatology, University of Tokyo Graduate School of Medicine, 7-3-1 Hongo, Bunkyo-ku, Tokyo 113-8655, Japan. yasano-tky@umin.ac.jp.

AUTHOR CONTRIBUTIONS

All authors were involved in drafting the article or revising it critically for important intellectual content, and all authors approved the final version to be published. Dr. Asano had full access to all of the data in the study and takes responsibility for the integrity of the data and the accuracy of the data analysis.

Study conception and design. Akamata, Asano, Sato.

Acquisition of data. Akamata, Asano, Noda, Takahashi, Ichimura, Toyama, Trojanowska.

Analysis and interpretation of data. Akamata, Asano, Yamashita, Taniguchi, Toyama, Trojanowska, Sato.

the mechanism underlying the beneficial effects of endothelin receptor blockade on SSc vasculopathy.

Systemic sclerosis (SSc) is a multisystem connective tissue disease characterized by immunologic abnormalities, vasculopathy, and resultant fibrosis of the skin and certain internal organs (1). Although the pathogenesis of SSc currently remains elusive, studies have demonstrated that bosentan, a dual endothelin receptor antagonist, prevents the development of new digital ulcers in SSc patients (2,3), suggesting a critical role of endothelin in the mechanism underlying SSc vasculopathy. The effect of bosentan on nailfold capillary changes is still up for debate, but previous studies have revealed that bosentan, alone or together with iloprost, fosters microvascular de-remodeling in nailfold capillaries (4–6), where morphologic changes mostly progress in parallel with disease duration and are refractory to canonical treatments such as prostanoids (5,7). These observations suggest that endothelin receptor blockade potentially has a disease-modifying impact on SSc vasculopathy.

Fli-1 is a member of the Ets family of transcription factors, which have been implicated in the development of fibrosis and vasculopathy associated with SSc. In dermal fibroblasts, Fli-1 functions as a potent repressor of the *COL1A1* and *COL1A2* genes (8–10), and its deficiency acts to coordinately modulate the expression of fibrosis-related genes toward the establishment of a profibrotic phenotype (11–13). Importantly, the expression of the *Fli1* gene is markedly decreased in lesional SSc skin and SSc dermal fibroblasts, at least partly as a result of epigenetic suppression at the transcription level (14). Fli-1 protein levels are also notably decreased in dermal microvascular endothelial cells of lesional SSc skin as compared with those of normal skin (15). Furthermore, endothelial cell–specific Fli-1–knockout (Fli-1 ECKO) mice exhibit the histologic and functional abnormalities characteristic of SSc vasculopathy, such as distortion of arterioles with thickened and occluded vascular walls and increased permeability of capillaries (16). These previous data suggest that Fli-1 down-regulation contributes to the establishment of an SSc phenotype in dermal fibroblasts and dermal microvascular endothelial cells and that the reversal of Fli-1 expression is a potential therapeutic strategy for SSc.

In a recent study we showed that bosentan reverses the profibrotic phenotype of SSc dermal fibroblasts by increasing the DNA binding ability and the expression levels of Fli-1 (17). Given that SSc vasculopathy at least partly results from endothelial Fli-1 deficiency (12,13,16,18), we reasoned that the effect of bosentan on digital ulcers and nailfold capillary changes in SSc may involve the normalization of Fli-1 expression levels in endothelial cells. To assess this hypothesis, we investigated the impact of endothelin 1 (ET-1) and bosentan on the behavior of Fli-1 in endothelial cells and the effect of bosentan on vascular abnormalities in Fli-1 ECKO mice, an animal model of SSc vasculopathy.

MATERIALS AND METHODS

Reagents

Anti–Fli-1 antibodies for immunoblotting and anti–protein kinase Cδ (anti-PKCδ) antibodies were purchased from Santa Cruz Biotechnology. Anti–Fli-1 antibodies for

immunohistochemistry were obtained from BD Biosciences. Antibodies against c-Abl and phospho–c-Abl (Tyr^{245}) were purchased from Cell Signaling Technology. Antibodies to β-actin were from Sigma-Aldrich. Polyclonal rabbit anti–phospho–Fli-1 (Thr^{312})–specific antibodies were generated as described previously (9). Bosentan was a gift from Actelion Pharmaceuticals.

Generation of Fli-1 ECKO mice

$Fli\text{-}1^{flx/flx}$ mice were generated as described previously (16). Mice expressing Cre recombinase under the control of the endothelium-specific tyrosine protein kinase receptor 2 promoter were purchased from The Jackson Laboratory and crossed with $Fli\text{-}1^{flx/flx}$ mice. Cre-mediated recombination of the flox allele in endothelial cells from different individual mice varied between 50% and 80% (16). All animal studies and procedures were approved by the Committee on Animal Experimentation of the University of Tokyo Graduate School of Medicine.

Cell culture

Human dermal microvascular endothelial cells (HDMECs) were purchased from Takara Bio. Murine dermal microvascular endothelial cells (MDMECs) were isolated from wild-type (WT) and Fli-1 ECKO mice. Briefly, newborn WT and Fli-1 ECKO mice (0–72 hours old) were killed by decapitation, rinsed in 70% ethanol, and the skin was removed. Excised mouse skin was placed in culture dishes dermis side down, with Dulbecco's modified Eagle's medium (DMEM) plus 3.5% Dispase (Sigma-Aldrich), and incubated at 4°C overnight. The dermis was separated from the epidermis, placed in DMEM plus 0.05% type I collagenase (Invitrogen), and incubated at 37°C for 1 hour. The cell suspension was filtered, centrifuged, stained with anti-CD31 microbeads (Miltenyi Biotec), and isolated using magnetic cell sorting. Isolation efficiency of MDMECs was decreased in Fli-1 ECKO mice as compared with WT mice, at least partially because of the decreased expression of CD31 on Fli-1–deficient mouse MDMECs as compared with WT mouse MDMECs (16). Endothelial cells were cultured on collagen-coated tissue culture plates in endothelial cell basal medium 2 (Cambrex) supplemented with endothelial cell growth media 2 SingleQuots (human vascular endothelial growth factor, epidermal growth factor, basic fibroblast growth factor, insulin-like growth factor 1, ascorbic acid, gentamicin, and heparin; Cambrex) and 5% heat-inactivated fetal bovine serum.

Cultured cells were assessed for a cobblestone appearance and specific staining for VE-cadherin and platelet endothelial cell adhesion molecule 1 (PECAM-1). Experiments were conducted with HDMECs and MDMECs at passages 1–3, in which a cobblestone appearance was maintained. Using a trypan blue exclusion test, we confirmed that ET-1 and bosentan at the concentrations used in this study did not affect the viability of HDMECs and/or MDMECs (data not shown).

Immunoblotting

Cells were grown to subconfluence and serum-starved when treated with the indicated reagents. Whole cell lysates and nuclear extracts were prepared as described previously (19,20). Samples were subjected to sodium dodecyl sulfate–polyacrylamide gel

electrophoresis and immunoblotting with the indicated primary antibodies. Bands were detected using enhanced chemiluminescence techniques (Thermo Scientific).

RNA isolation and real-time quantitative reverse transcription–polymerase chain reaction (qRT-PCR)

Total RNA was isolated from cultured endothelial cells with RNeasy spin columns (Qiagen). One microgram of total RNA from each sample was reverse transcribed into complementary DNA using the iScript cDNA Synthesis kit (Bio-Rad). Real-time qRT-PCR was performed using Fast SYBR Green PCR Master Mix (Applied Biosystems) on an ABI Prism 7000 (Applied Biosystems) in triplicate. The sequences of primers for Fli-1 and 18S ribosomal RNA (rRNA) were as follows: for human Fli-1, forward 5′-GGATGGCAAGGAACTGTGTAA-3′ and reverse 5′-GGTTGTATAGGCCAGCAG-3′; for mouse Fli-1, forward 5′-ACTTGGCCAAATGGACGGGACTAT-3′ and reverse 5′-CCCGTAGTCAGGACTCCCG-3′; for human 18S rRNA, forward 5′-CGCCGCTAGAGGTGAAATTC-3′ and reverse 5′-TTGGCAAATGCTTTCGCTC-3′; and for mouse 18S rRNA, forward 5′-CGCCGCTAGAGGTGAAA TTC-3′ and reverse 5′-TTGGCAAATGCTTTCGCTC-3′. The $\Delta\Delta C_t$ method was used to compare target gene and housekeeping gene (18S rRNA) messenger RNA (mRNA) expression.

Chromatin immunoprecipitation (ChIP) assay

ChIP assay was performed using an EpiQuik ChIP kit (Epigentek). Briefly, cells were treated with 1% formaldehyde for 10 minutes. The crosslinked chromatin was then prepared and sonicated to an average size of 300–500 bp. The DNA fragments were immunoprecipitated with anti–Fli-1 antibody at 4°C. As a negative control, normal rabbit IgG was used. After reversal of crosslinking, the immunoprecipitated chromatin was quantified by qRT-PCR. Primer sequences for the promoters of murine target genes, including *Cdh5*, *Pecam1*, *Pdgfb*, and *Mmp9*, have been described previously (16). Primer sequences for the promoters of human target genes were as follows: for VE-cadherin/F-1493, 5′-ACAAAGGGAATTGGCAGATG-3′ and for VE-cadherin/R-1319, 5′-AGTGCTCTGTCCCCTGTGTT-3′; for PECAM-1/F-1039, 5′-GGCCCCAAAGGTCAATCTTA-3′ and for PECAM-1/R-820, 5′-GGGCAACAGAGTGAGACTCC-3′; for platelet-derived growth factor β (PDGFβ)/F-1371, 5′-GCTGGGACTACAGGAGCTTG-3′ and for PDGFβ/R-1216, 5′-CATCACCTTGGTCCAAATCC-3′; for matrix metalloproteinase 9 (MMP-9)/F-353, 5′-CTGGAGGCTTTCAGACCAAG-3′ and for MMP-9/R-150, 5′-AAGGGCTTACACCACCTCCT-3′. Using electrophoresis, we confirmed the presence of 175 bp, 220 bp, 156 bp, 204 bp, 183 bp, 246 bp, 171 bp, and 204 bp amplicons for the promoters of the *CDH5*, *PECAM1*, *PDGFB*, *MMP9*, *Cdh5*, *Pecam1*, *Pdgfb*, and *Mmp9* genes, respectively. No nonspecific amplification was detected in these experiments.

Administration of bosentan to mice

Isoflurane-anesthetized mice (8 weeks old) were infused with bosentan (sodium salt; 20 mg/kg) in 200 μl of 0.9% saline intraperitoneally for 28 days continuously.

Immunohistochemistry

Immunohistochemistry analysis with a Vectastain ABC kit (Vector) was performed on formalin-fixed, paraffin-embedded tissue sections using antibodies against Fli-1 and α-smooth muscle actin (α-SMA) according to the manufacturer's instructions.

Vascular permeability assay

Evans blue dye (0.5%) in 200 μl of 0.9% saline was injected into the tail vein and animals were killed after 30 minutes. Intravascular Evans blue dye was removed by flushing the systemic vasculature with 30 ml of saline through a cannula placed in the aorta. The presence of vascular leakage was macroscopically evaluated in the skin.

Visualization of the dermal vascular structure by fluorescein isothiocyanate (FITC)–conjugated dextran injection

Mice were anesthetized, and 200 μl of FITC-conjugated dextran (2,000 kd [20 mg/ml in phosphate buffered saline]) was injected into the tail vein. After 5 minutes, mice were killed, and a full-thickness specimen of back skin (4 × 2 cm) was prepared. The skin specimen was placed directly on the slide (epidermis side up), and the structure of vascular network in the skin was visualized by fluorescence microscopy.

Statistical analysis

Statistical analysis was performed using one-way analysis of variance (ANOVA) followed by Tukey's post hoc test for multiple comparisons and Mann-Whitney U test for 2-group comparisons. A paired *t*-test was used for the comparison of normally distributed paired data. *P* values less than 0.05 were considered significant.

RESULTS

ET-1 regulates the transcriptional activity of Fli-1 in HDMECs

Since ET-1 regulates the transcriptional activity of Fli-1 in dermal fibroblasts (17), we initially investigated whether it affects the transcriptional activity of Fli-1 in HDMECs. Our previous studies have demonstrated that transcriptional activity of Fli-1 is tightly regulated by the phosphorylation/acetylation cascade triggered by the PKCδ-dependent phosphorylation of Fli-1 at Thr^{312} (9). Phosphorylated Fli-1 is subsequently acetylated by p300/CREB binding protein–associated factor at Lys^{380}, resulting in a loss of DNA binding ability and subsequent degradation (8). Since the phosphorylation of Fli-1 at Thr^{312} is a critical step in the regulation of Fli-1 transcriptional activity, we examined the effect of ET-1 on the phosphorylation levels of Fli-1 at Thr^{312}.

As shown in Figure 1A, consistent with our hypothesis, after 24 hours of ET-1 stimulation levels of Fli-1 phosphorylation at Thr^{312} were increased, while its total protein levels were decreased, in a dose-dependent manner (the mean ± SEM ratio of phospho–Fli-1 to total Fli-1 as compared with baseline was 2.76 ± 0.43, 9.05 ± 1.07, and 7.85 ± 1.26 with 50 n*M*, 100 n*M*, and 200 n*M* of ET-1, respectively; $P = 0.0004$ by one-way ANOVA, $P < 0.05$ for baseline versus 100 n*M* or 200 n*M* of ET-1 by Tukey's post hoc test). In contrast, ET-1 did not alter levels of mRNA for the *Fli1* gene under the same conditions (the mean ± SEM

relative expression level of Fli-1 mRNA as compared with baseline was 0.96 ± 0.10, 0.90 ± 0.06, and 1.00 ± 0.17 with 50 n*M*, 100 n*M*, and 200 n*M* of ET-1, respectively; $P = 0.88$ by one-way ANOVA) (Figure 1B). These results suggest that ET-1 induces Fli-1 phosphorylation at Thr^{312}, leading to the decrease in Fli-1 protein levels through degradation, which is consistent with the previous observation in dermal fibroblasts (17). Since ET-1 at 200 n*M* did not affect the viability of HDMECs evaluated by trypan blue exclusion test (data not shown), we used 200 n*M* of ET-1 in the subsequent experiments.

To further investigate whether ET-1 decreases binding of Fli-1 to the target gene promoters, we used ChIP analysis. Since Fli-1 binds to the promoters of the *CDH5*, *PECAM1*, *PDGFB*, and *MMP9* genes and directly modulates their expression (16), we assessed the binding of Fli-1 to the promoter region of these genes. As shown in Figure 1C, ET-1 decreased the binding of Fli-1 to the target gene promoters at 2 hours (the mean ± SEM relative pulldown by Fli-1 compared to IgG was 1.00 ± 0.11 at baseline versus 0.12 ± 0.03 after ET-1 stimulation, 1.00 ± 0.60 at baseline versus 0.02 ± 0.01 after ET-1 stimulation, 1.00 ± 0.10 at baseline versus 0.13 ± 0.02 after ET-1 stimulation, and 1.00 ± 0.17 at baseline versus 0.09 ± 0.04 after ET-1 stimulation for the promoters of *CDH5*, *PDGFB*, *PECAM1*,and *MMP9*, respectively; $P < 0.05$ for all by Mann-Whitney U test). Collectively, these results indicate that ET-1 decreases the DNA binding ability of Fli-1 in HDMECs.

Activation of the c-Abl/PKCδ/Fli-1 pathway in HDMECs by ET-1

We next investigated whether ET-1 activates the c-Abl/PKCδ/Fli-1 pathway in HDMECs. Since ET-1 increases the expression levels of c-Abl and PKCδ in dermal fibroblasts, we first explored its effect on the expression levels of c-Abl and PKCδ in HDMECs. As shown in Figure 2A, as expected, ET-1 stimulation increased the expression levels of c-Abl and PKCδ as early as 15 minutes. Given that the nuclear translocation of PKCδ reflects its activation status, we also evaluated nuclear localization of PKCδ. Consistent with our expectations, ET-1 promoted the nuclear translocation of PKCδ (Figure 2B). To further confirm that c-Abl activation sequentially induces PKCδ activation and Fli-1 phosphorylation, we examined the effect of small interfering RNA (siRNA) against c-Abl or PKCδ on the expression levels of c-Abl and PKCδ and the phosphorylation levels of Fli-1 induced by ET-1. As shown in Figure 2C, c-Abl siRNA inhibited PKCδ induction and Fli-1 phosphorylation, while PKCδ siRNA attenuated Fli-1 phosphorylation, but not c-Abl induction. These results indicate that c-Abl is required for ET-1–dependent PKCδ activation, consistent with sequential activation of the c-Abl/PKCδ/Fli-1 pathway in HDMECs as well as in dermal fibroblasts.

Bosentan suppresses the c-Abl/PKCδ/Fli-1 pathway by inhibiting autocrine endothelin signaling in HDMECs

Since endothelin is an autocrine/paracrine peptide (mainly produced by endothelial cells) that is indispensable in the maintenance of vascular homeostasis in vivo, we next examined the role of autocrine endothelin in the regulation of the DNA binding ability of Fli-1 in HDMECs. To this end, we used a dual endothelin receptor antagonist, bosentan, and investigated its effect on the c-Abl/PKCδ/Fli-1 pathway in HDMECs. Since bosentan at 10, 20, and 40 μ*M* did not affect the viability of HDMECs evaluated by trypan blue exclusion test (data not shown), we used 20 μ*M* of bosentan in the subsequent experiments. As shown

in Figures 3A and B, bosentan suppressed the expression of the c-Abl and PKCδ proteins, the phosphorylation levels of Fli-1, and the nuclear localization of PKCδ, while increasing Fli-1 protein levels, in HDMECs. Collectively, these results indicate that the autocrine endothelin pathway regulates the transcriptional activity of Fli-1 in HDMECs.

Four weeks of treatment with bosentan alleviates vascular fragility, but not abnormal vascular structure, in Fli-1 ECKO mice by increasing endothelial Fli-1 expression

In order to investigate the effect of bosentan on the expression levels of Fli-1 in endothelial cells in vivo, bosentan (20 mg/kg) was given intraperitoneally to Fli-1 ECKO mice and WT mice for 4 weeks (this did not affect the viability of bleomycin-treated mice in our previous study [17]), and Fli-1 protein levels were determined by immunohistochemistry analysis. As shown in Figure 4A, Fli-1 was expressed abundantly in dermal microvascular endothelial cells of WT mice treated with saline, while Fli-1 expression levels were highly variable in dermal microvascular endothelial cells of saline-treated Fli-1 ECKO mice due to the variable efficiency of the Cre enzyme in individual endothelial cells (data available upon request from the corresponding author). After treatement with bosentan, the expression levels of Fli-1 protein were substantially increased in endothelial cells of Fli-1 ECKO mice, while the abundant expression of Fli-1 in endothelial cells of WT mice was not altered after the treatment. These results indicate that bosentan increases Fli-1 protein levels in dermal microvascular endothelial cells in vivo.

As previously reported, Fli-1 ECKO mice exhibit the structural and functional abnormalities of SSc vasculopathy, including distortion of arterioles with thickened and occluded vascular walls and increased vascular permeability due to fragile capillaries (16). To investigate the effect of bosentan on vasculopathy of Fli-1 ECKO mice, we first compared vascular permeability by injecting Evans blue dye into mice treated with either bosentan or saline.

As shown in Figure 4B, consistent with results of a previous study (16), extensive vascular leakage was observed in the skin of saline-treated Fli-1 ECKO mice, but not saline-treated WT mice. In contrast, vascular leakage was greatly diminished in Fli-1 ECKO mice that were treated with bosentan for 4 weeks. Since the altered phenotype of pericytes is closely related to vascular fragility of capillaries, leading to increased vascular permeability (16,21), we also investigated expression levels of α-SMA, a marker of pericytes closely interacting with endothelial cells, i.e., vascular stabilization. Consistent with results of a previous study (16), α-SMA expression was markedly decreased in dermal small vessels of Fli-1 ECKO mice treated with saline when compared to dermal blood vessels of saline-treated WT mice (Figure 4C). After 4 weeks of bosentan treatment, α-SMA expression was increased in dermal small vessels of Fli-1 ECKO mice, suggesting that bosentan promotes vascular stabilization in these mice.

We next examined the effect of bosentan on vascular structure, as visualized by FITC-conjugated dextran injection. As shown in Figure 4D, vascular distortion was evident in saline-treated Fli-1 ECKO mice, while vascular structure was well-organized in saline-treated WT mice. After 4 weeks of bosentan treatment, in contrast to the results seen with injection of Evans blue dye, no notable difference was seen in the vascular structure of WT and Fli-1 ECKO mice as compared to saline-treated control mice. Since this technique

cannot be used to evaluate microcirculation corresponding to human nailfold capillaries, the effect of bosentan on the morphology of microvasculature in Fli-1 ECKO mice remains unclear.

To further confirm the effect of bosentan on dermal microvascular endothelial cells in Fli-1 ECKO mice, we isolated MDMECs from Fli-1 ECKO mice and treated them with bosentan for 48 hours. As shown in Figures 5A and B, bosentan increased Fli-1 protein levels, with a dose-dependent decrease of the ratio of phospho–Fli-1 to total Fli-1 (the mean ± SEM ratio of phospho–Fli-1 to total Fli-1 compared with baseline was 0.61 ± 0.09, 0.43 ± 0.15, and 0.24 ± 0.05 with 10 μ*M*, 20 μ*M*, and 40 μ*M* of bosentan, respectively; $P = 0.0034$ by one-way ANOVA, $P < 0.05$ for baseline versus 20 or 40 μ*M* of bosentan by Tukey's post hoc test) (Figure 5A), but not Fli-1 mRNA levels (the mean ± SEM relative expression level of Fli-1 mRNA compared with baseline was 0.91 ± 0.14, 1.05 ± 0.13, and 1.05 ± 0.11 with 10 μ*M*, 20 μ*M*, and 40 μ*M* of bosentan, respectively; $P = 0.80$ by one-way ANOVA) (Figure 5B), suggesting that bosentan alters Fli-1 levels by inhibiting its degradation.

The binding of Fli-1 to target gene promoters in MDMECs was also markedly magnified by bosentan (the mean ± SEM relative pulldown by Fli-1 compared to IgG was 1.00 ± 0.24 at baseline versus 13.50 ± 4.22 after bosentan treatment, 1.00 ± 0.40 at baseline versus 4.58 ± 1.04 after bosentan treatment, 1.00 ± 0.33 at baseline versus 14.50 ± 6.84 after bosentan treatment, and 1.00 ± 0.28 at baseline versus 9.19 ± 2.86 after bosentan treatment for the promoters of *Cdh5*, *Pdgfb*, *Pecam1*, and *Mmp9*, respectively; $P < 0.05$ for all by Mann-Whitney U test) (Figure 5C). Collectively, these results indicate that bosentan reverses Fli-1 deficiency–dependent vasculopathy by increasing the transcriptional activity of Fli-1.

DISCUSSION

This study was based on the hypothesis that bosentan augments the transcriptional activity of Fli-1 by increasing its expression and DNA binding ability in endothelial cells. In support of our hypothesis, in HDMECs, ET-1 activated the c-Abl/PKCδ/Fli-1 pathway, leading to a decrease in expression levels and promoter binding ability of Fli-1, and bosentan augmented the transcriptional activity of Fli-1 by increasing its expression and promoter binding ability through the blockade of autocrine endothelin. Given that blockade of the c-Abl/PKCδ/Fli-1 pathway increases the protein levels of Fli-1 by increasing its protein stability while not affecting its mRNA levels (8,9,22), bosentan would theoretically be able to increase levels of Fli-1 protein in endothelial cells of Fli-1 ECKO mice (in which endothelial Fli-1 expression is reduced by 50–80% due to Cre-mediated deletion of the floxed sequences in the *Fli1* gene) (16). Consistent with this hypothesis, in Fli-1 ECKO mice, 4 weeks of treatment with bosentan increased the protein levels of Fli-1 in dermal microvascular endothelial cells and improved vascular leakage by promoting vascular stabilization characterized by α-SMA expression in pericytes. Collectively, these results indicate that the ET-1 signaling pathway targets Fli-1 in endothelial cells, and bosentan reverses some of the vascular defects related to endothelial Fli-1 deficiency in animal models.

SSc vasculopathy is believed to be caused by aberrant vascular remodeling due to impaired angiogenesis and vasculogenesis, the molecular mechanism of which still remains unclear

(23,24). In the dermal microvessels of lesional SSc skin, the expression of α-SMA, a marker of pericytes with an angiostatic phenotype, is decreased (16), while the expression of regulator of G protein signaling 5, a marker of pericytes with an angiogenic phenotype, is elevated (25). This phenotypic change of pericytes suggests that SSc dermal microvessels are unstable and fragile with proangiogenic properties, probably reflecting a compensatory response in order to maintain vascular function. Vascular destabilization in SSc is attributable to the down-regulation of molecules relevant to vascular stabilization, such as VE-cadherin, PECAM-1, and PDGFβ, and the up-regulation of the enzyme that degrades vascular basement membrane, MMP-9. Importantly, the altered expression of these molecules is recapitulated in dermal blood vessels of Fli-1 ECKO mice (16).

Furthermore, the expression profile of angiogenesis-related molecules, including cathepsin V, cathepsin B, and CXCL5, in SSc dermal blood vessels is also reproduced in Fli-1 ECKO mice (12,13,18). Considering that Fli-1 ECKO mice are characterized by leaky and fragile capillaries and thickened and occluded arterioles similar to those seen in SSc (16), Fli-1 deficiency may largely contribute to the induction of the SSc vascular phenotype. Epigenetic suppression has previously been implicated in the mechanism causing Fli-1 deficiency in SSc (14), but results of the present study suggest that ET-1 may also be involved in the down-regulation of Fli-1 in SSc dermal microvascular endothelial cells. This notion is consistent with the previous clinical observation that circulating ET-1 levels are elevated in SSc patients with the diffuse cutaneous involvement that usually accompanies extensive microangiopathy and severe vascular complications, such as pulmonary arterial hypertension and scleroderma renal crisis (26–28).

Since Fli-1 is a potential predisposing factor in SSc (29,30), the normalization of Fli-1 expression may partially improve clinical symptoms of this disease. Given that Fli-1 has been shown to be epigenetically suppressed in SSc skin and dermal fibroblasts (14), the use of epigenetic inhibitors to restore Fli-1 levels may be a potential therapeutic strategy for SSc. However, the systemic administration of epigenetic inhibitors raises serious concerns related to the nonspecific activation of unrelated genes. On the other hand, bosentan has a unique property that augments Fli-1 protein levels even in cells with genetically reduced Fli-1 mRNA levels, as has been demonstrated in Fli-1 ECKO mice. Therefore, bosentan is capable of increasing Fli-1 protein levels even though its expression is strongly suppressed by an epigenetic mechanism, suggesting that endothelin receptor blockade has a potential therapeutic impact on SSc vasculopathy beyond the reversal of the pathologic effects of ET. This theory is consistent with prior reported clinical data. For example, 1 year of treatment with bosentan, but not iloprost, increases the number of nailfold capillaries with early and active patterns (i.e., enlarged capillaries, megacapillaries, and hemorrhages) and decreases the number of nailfold capillaries with late patterns (i.e., capillary loss, ramified capillaries, and capillary disorganization) (4). Furthermore, 3 years of combination therapy with bosentan and iloprost increases the number of nailfold capillaries, while iloprost alone results in a significant decrease in the number of nailfold capillaries (5). Importantly, the beneficial effect of bosentan on SSc vasculopathy was only modest and limited in these studies (a reasonable result since Fli-1 deficiency is one of the predisposing factors in this disease).

As shown in the RAPIDS-1 and RAPIDS-2 studies (Randomized Placebo-controlled studies on prevention of Ischemic Digital ulcers in Scleroderma), bosentan prevents the development of new digital ulcers in SSc without having an effect on healing of preexisting digital ulcers (2,3). The presence of ulnar artery occlusion is closely related to new or recurrent onset of digital ulcers in SSc (31). Since ET-1 plays a critical role in the development of proliferative obliterative vasculopathy by inducing fibroproliferative changes in the vessel wall (32,33), bosentan has been believed to elicit a significant preventive effect on digital ulcers by improving peripheral circulation through a potential reverse remodeling effect as well as a potent vasodilatory effect. On the other hand, ET-1 also plays a part in pathologically activated angiogenesis. For instance, bosentan alleviates increased neovascularization and leaky vessels in the cerebrovascular system in an animal model of type 2 diabetes and inhibits tumor vascularization and bone metastasis in an animal model of breast carcinoma cell metastasis (34,35). This is also the case in SSc, since, as noted above, the number of nailfold ramified capillaries (a reflection of activated angiogenesis) has been found to be decreased after 1 year of treatment with bosentan (4).

As a result of its dual, conflicting effects on SSc vasculopathy (the improvement of peripheral circulation and the inhibition of angiogenesis), bosentan would not be expected to have a beneficial impact on preexisting digital ulcers in SSc (2,3). However, as reported by Cutolo et al (5), combination therapy with bosentan and iloprost, but not iloprost alone, increases the number of nailfold ramified capillaries, suggesting that combination therapy, but neither bosentan nor iloprost alone, promotes angiogenesis. Although combination therapy with bosentan and prostanoids was not allowed in the RAPIDS-1 and RAPIDS-2 studies, combination therapy may promote angiogenesis in SSc, potentially leading to a beneficial effect on digital ulcers, in which the normalization of Fli-1 protein expression in endothelial cells may be involved. To address this issue, further studies are under way in our laboratory. Although the reported clinical effect of bosentan described above is at best marginal, the elucidation of its molecular mechanism provides us with a useful clue for the further development of therapeutic strategies for SSc vasculopathy.

In summary, this is the first report to demonstrate a possible molecular basis for the impact of endothelin receptor blockade on SSc vasculopathy. Normalization of the expression levels of a potential predisposing factor of SSc (the transcription factor Fli-1) strongly indicates that the combination of bosentan with conventional therapies may ameliorate a broad spectrum of pathologic processes in SSc.

Acknowledgments

Supported by the Ministry of Health, Labor, and Welfare of Japan (grants to Drs. Asano and Sato), the Japan Intractable Diseases Research Foundation, a Rohto Dermatology Prize, the Japanese Society for Investigative Dermatology Fellowship Shiseido Award, the Mochida Memorial Foundation for Medical and Pharmaceutical Research, and an Actelion Academia Award (to Dr. Asano). Dr. Trojanowska's work was supported by the NIH (grant AR-042334).

Dr. Asano has received honoraria (less than $10,000) as well as research funding from Actelion.

References

1. Asano Y. Future treatments in systemic sclerosis. J Dermatol. 2010; 37:54–70. [PubMed: 20175840]

2. Korn JH, Mayes M, Matucci Cerinic M, Rainisio M, Pope J, Hachulla E, et al. for the RAPIDS-1 Study Group. Digital ulcers in systemic sclerosis: prevention by treatment with bosentan, an oral endothelin receptor antagonist. Arthritis Rheum. 2004; 50:3985–3993. [PubMed: 15593188]
3. Matucci-Cerinic M, Denton CP, Furst DE, Mayes MD, Hsu VM, Carpentier P, et al. Bosentan treatment of digital ulcers related to systemic sclerosis: results from the RAPIDS-2 randomised, double-blind, placebo-controlled trial. Ann Rheum Dis. 2011; 70:32–38. [PubMed: 20805294]
4. Guiducci S, Bellando Randone S, Bruni C, Carnesecchi G, Maresta A, Iannone F, et al. Bosentan fosters microvascular de-remodelling in systemic sclerosis. Clin Rheumatol. 2012; 31:1723–1725. [PubMed: 23053682]
5. Cutolo M, Zampogna G, Vremis L, Smith V, Pizzorni C, Sulli A. Longterm effects of endothelin receptor antagonism on microvascular damage evaluated by nailfold capillaroscopic analysis in systemic sclerosis. J Rheumatol. 2013; 40:40–45. [PubMed: 23118114]
6. Hettema ME, Zhang D, Stienstra Y, Smit AJ, Bootsma H, Kallenberg CG. No effects of bosentan on microvasculature in patients with limited cutaneous systemic sclerosis. Clin Rheumatol. 2009; 28:825–833. [PubMed: 19350343]
7. Shah P, Murray AK, Moore TL, Herrick AL. Effects of iloprost on microvascular structure assessed by nailfold videocapillaroscopy: a pilot study. J Rheumatol. 2011; 38:2079–2080. [PubMed: 21885525]
8. Asano Y, Czuwara J, Trojanowska M. Transforming growth factor-β regulates DNA binding activity of transcription factor Fli1 by p300/CREB-binding protein-associated factor-dependent acetylation. J Biol Chem. 2007; 282:34672–34683. [PubMed: 17884818]
9. Asano Y, Trojanowska M. Phosphorylation of Fli1 at threonine 312 by protein kinase C δ promotes its interaction with p300/CREB-binding protein-associated factor and subsequent acetylation in response to transforming growth factor β. Mol Cell Biol. 2009; 29:1882–1894. [PubMed: 19158279]
10. Asano Y, Trojanowska M. Fli1 represses transcription of the human α2(I) collagen gene by recruitment of the HDAC1/p300 complex. PLoS One. 2013; 8:e74930. [PubMed: 24058639]
11. Nakerakanti SS, Kapanadze B, Yamasaki M, Markiewicz M, Trojanowska M. Fli1 and Ets1 have distinct roles in connective tissue growth factor/CCN2 gene regulation and induction of the profibrotic gene program. J Biol Chem. 2006; 281:25259–25269. [PubMed: 16829517]
12. Noda S, Asano Y, Akamata K, Aozasa N, Taniguchi T, Takahashi T, et al. A possible contribution of altered cathepsin B expression to the development of skin sclerosis and vasculopathy in systemic sclerosis. PLoS One. 2012; 7:e32272. [PubMed: 22384200]
13. Noda S, Asano Y, Takahashi T, Akamata K, Aozasa N, Taniguchi T, et al. Decreased cathepsin V expression due to Fli1 deficiency contributes to the development of dermal fibrosis and proliferative vasculopathy in systemic sclerosis. Rheumatology (Oxford). 2013; 52:790–799. [PubMed: 23287360]
14. Wang Y, Fan PS, Kahaleh B. Association between enhanced type I collagen expression and epigenetic repression of the FLI1 gene in scleroderma fibroblasts. Arthritis Rheum. 2006; 54:2271–2279. [PubMed: 16802366]
15. Kubo M, Czuwara-Ladykowska J, Moussa O, Markiewicz M, Smith E, Silver RM, et al. Persistent down-regulation of Fli1, a suppressor of collagen transcription, in fibrotic scleroderma skin. Am J Pathol. 2003; 163:571–581. [PubMed: 12875977]
16. Asano Y, Stawski L, Hant F, Highland K, Silver R, Szalai G, et al. Endothelial Fli1 deficiency impairs vascular homeostasis: a role in scleroderma vasculopathy. Am J Pathol. 2010; 176:1983–1998. [PubMed: 20228226]
17. Akamata K, Asano Y, Aozasa N, Noda S, Taniguchi T, Takahashi T, et al. Bosentan reverses the pro-fibrotic phenotype of systemic sclerosis dermal fibroblasts via increasing DNA binding ability of transcription factor Fli1. Arthritis Res Ther. 2014; 16:R86. [PubMed: 24708674]
18. Ichimura Y, Asano Y, Akamata K, Takahashi T, Noda S, Taniguchi T, et al. Fli1 deficiency contributes to the suppression of endothelial CXCL5 expression in systemic sclerosis. Arch Dermatol Res. 2014; 306:331–338. [PubMed: 24292093]
19. Asano Y, Ihn H, Yamane K, Kubo M, Tamaki K. Increased expression levels of integrin αVβ5 on scleroderma fibroblasts. Am J Pathol. 2004; 164:1275–1292. [PubMed: 15039216]

20. Ihn H, Tamaki K. Competition analysis of the human α2(I) collagen promoter using synthetic oligonucleotides. J Invest Dermatol. 2000; 114:1011–1016. [PubMed: 10771485]
21. Von Tell D, Armulik A, Betsholtz C. Pericytes and vascular stability. Exp Cell Res. 2006; 312:623–629. [PubMed: 16303125]
22. Bujor AM, Asano Y, Haines P, Lafyatis R, Trojanowska M. The c-Abl tyrosine kinase controls protein kinase Cδ–induced Fli-1 phosphorylation in human dermal fibroblasts. Arthritis Rheum. 2011; 63:1729–1737. [PubMed: 21321929]
23. Distler JH, Gay S, Distler O. Angiogenesis and vasculogenesis in systemic sclerosis. Rheumatology (Oxford). 2006; 45(Suppl 3):iii26–iii27. [PubMed: 16987827]
24. Rabquer BJ, Koch AE. Angiogenesis and vasculopathy in systemic sclerosis: evolving concepts. Curr Rheumatol Rep. 2012; 14:56–63. [PubMed: 22083296]
25. Fleming JN, Nash RA, McLeod DO, Fiorentino DF, Shulman HM, Connolly MK, et al. Capillary regeneration in scleroderma: stem cell therapy reverses phenotype? PLoS One. 2008; 3:e1452. [PubMed: 18197262]
26. Yamane K, Miyauchi T, Suzuki N, Yuhara T, Akama T, Suzuki H, et al. Significance of plasma endothelin-1 levels in patients with systemic sclerosis. J Rheumatol. 1992; 19:1566–1571. [PubMed: 1464869]
27. Vancheeswaran R, Magoulas T, Efrat G, Wheeler-Jones C, Olsen I, Penny R, et al. Circulating endothelin-1 levels in systemic sclerosis subsets: a marker of fibrosis or vascular dysfunction? J Rheumatol. 1994; 21:1838–1844. [PubMed: 7837147]
28. Penn H, Quillinan N, Khan K, Chakravarty K, Ong VH, Burns A, et al. Targeting the endothelin axis in scleroderma renal crisis: rationale and feasibility. QJM. 2013; 106:839–848. [PubMed: 23696678]
29. Asano Y, Bujor AM, Trojanowska M. The impact of Fli1 deficiency on the pathogenesis of systemic sclerosis. J Dermatol Sci. 2010; 59:153–162. [PubMed: 20663647]
30. Mayes MD, Trojanowska M. Genetic factors in systemic sclerosis. Arthritis Res Ther. 2007; 9(Suppl 2):S5. [PubMed: 17767743]
31. Frerix M, Stegbauer J, Dragun D, Kreuter A, Weiner SM. Ulnar artery occlusion is predictive of digital ulcers in SSc: a duplex sonography study. Rheumatology (Oxford). 2012; 51:735–742. [PubMed: 22190687]
32. Hasegawa M, Nagai Y, Tamura A, Ishikawa O. Arteriographic evaluation of vascular changes of the extremities in patients with systemic sclerosis. Br J Dermatol. 2006; 155:1159–1164. [PubMed: 17107383]
33. Ichimura Y, Asano Y, Hatano M, Tamaki Z, Takekoshi T, Kogure A, et al. Significant attenuation of macrovascular involvement by bosentan in a patient with diffuse cutaneous systemic sclerosis with multiple digital ulcers and gangrene. Mod Rheumatol. 2011; 21:548–552. [PubMed: 21547701]
34. Abdelsaid M, Kaczmarek J, Coucha M, Ergul A. Dual endothelin receptor antagonism with bosentan reverses established vascular remodeling and dysfunctional angiogenesis in diabetic rats: relevance to glycemic control. Life Sci. 2014; 118:268–273. [PubMed: 24447630]
35. Dreau D, Karaa A, Culberson C, Wyan H, McKillop IH, Clemens MG. Bosentan inhibits tumor vascularization and bone metastasis in an immunocompetent skin-fold chamber model of breast carcinoma cell metastasis. Clin Exp Metastasis. 2006; 23:41–53. [PubMed: 16826430]

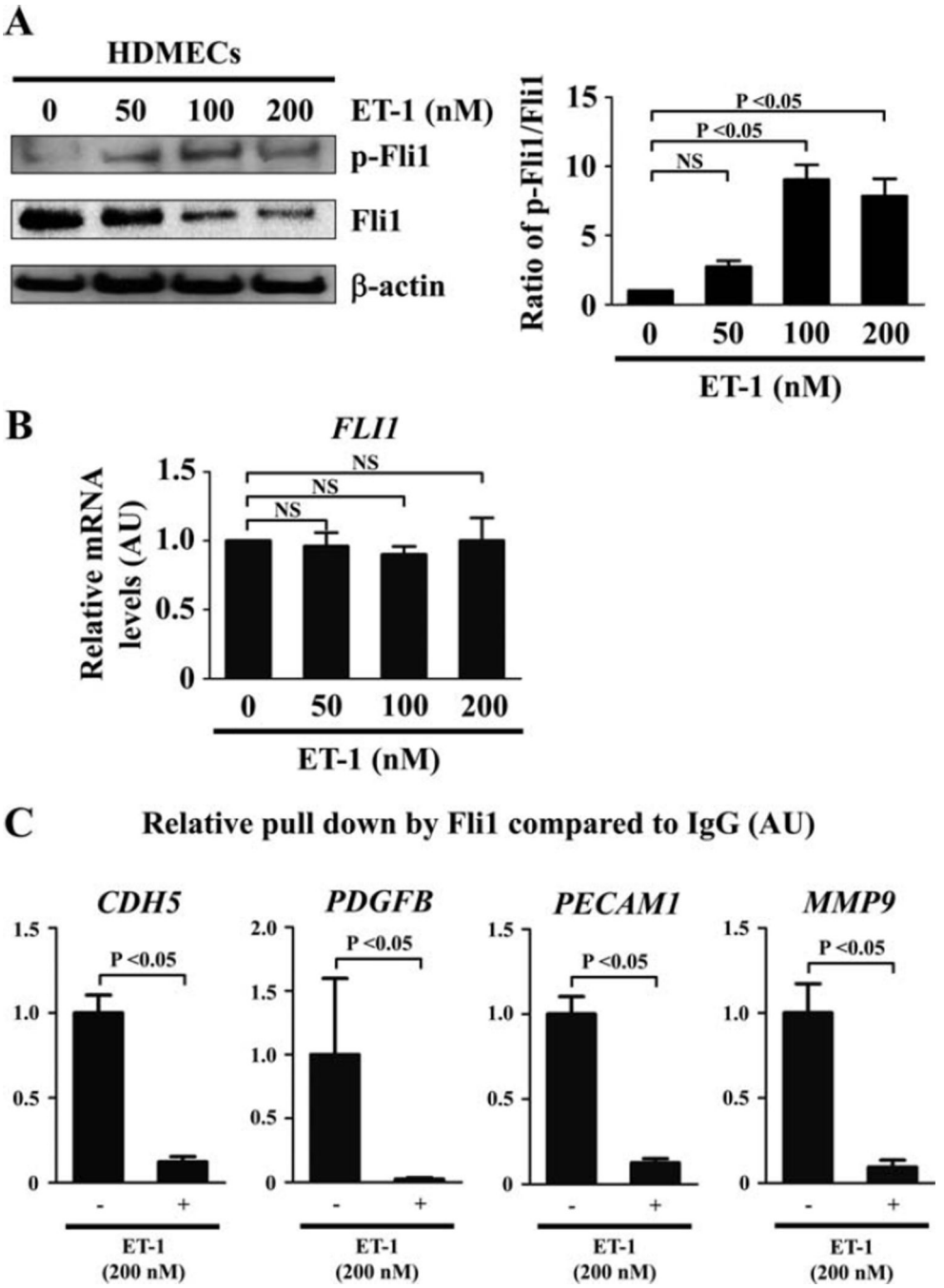

Figure 1.

Effect of endothelin 1 (ET-1) on Fli-1 expression and function in human dermal microvascular endothelial cells (HDMECs). **A**, HDMECs were treated for 24 hours with ET-1 at the indicated concentrations, and the expression and phosphorylation levels of Fli-1 were determined by immunoblotting with whole cell lysates (β-actin was used as a control for equal loading). The fold change in the ratio of phospho–Fli-1 to total Fli-1 (quantified by densitometry) was determined. **B**, Levels of mRNA for Fli-1 after the same treatment as described in **A** were evaluated by quantitative reverse transcription–polymerase chain

reaction (qRT-PCR). **C**, HDMECs were treated with ET-1 (200 n*M*) or vehicle for 2 hours and analyzed by chromatin immunoprecipitation. The binding of Fli-1 to the target gene promoters (*CDH5*, *PDGFB*, *PECAM1*, and *MMP9*) in response to ET-1 as compared to unstimulated controls (set at 1) was quantified by qRT-PCR. Values are the mean ± SEM (n = 3 mice per group). NS = not significant.

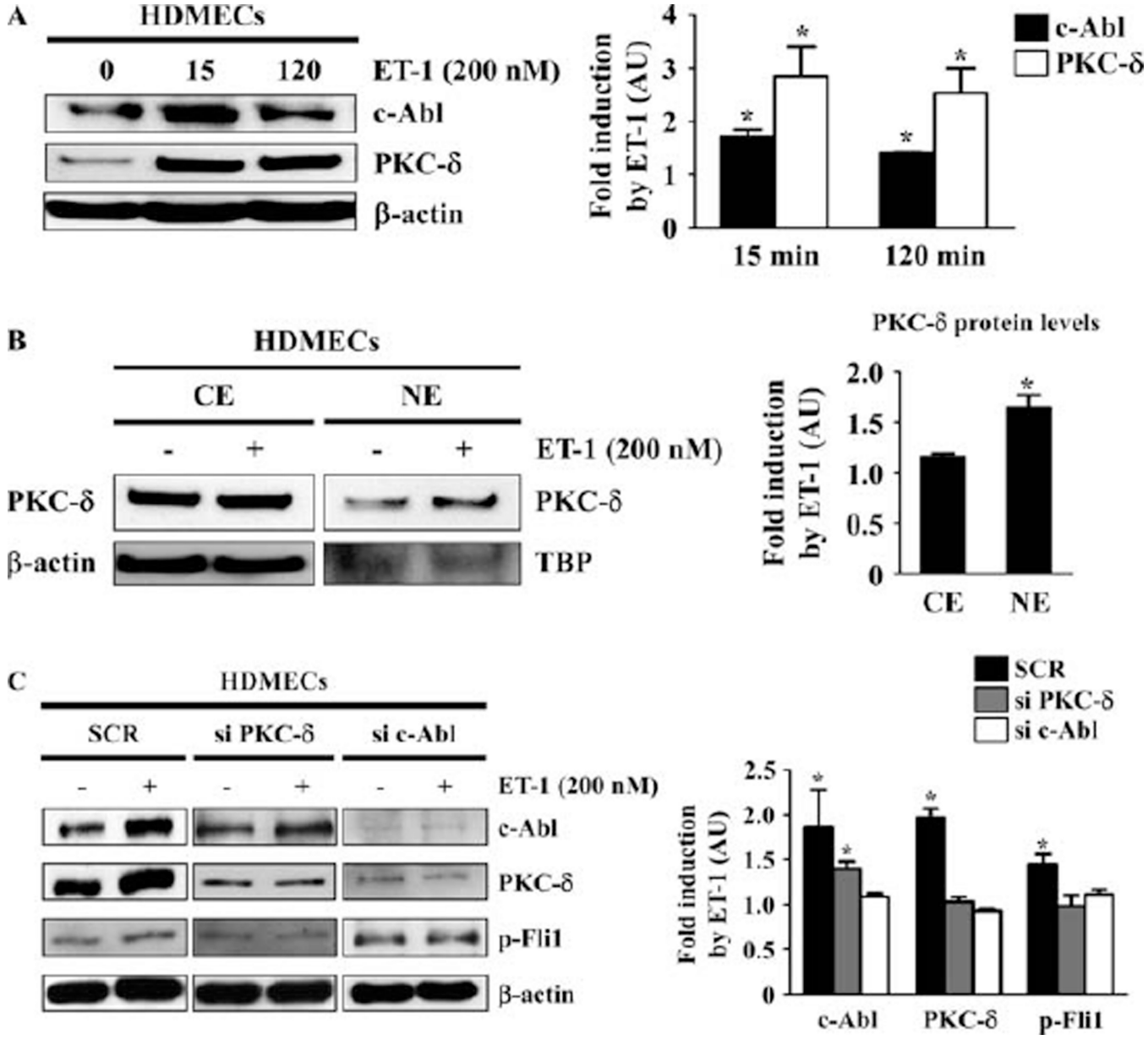

Figure 2.

Endothelin 1 (ET-1) activates the c-Abl/protein kinase Cδ (PKCδ)/Fli-1 pathway in human dermal microvascular endothelial cells (HDMECs). **A**, HDMECs were treated with ET-1 (200 n*M*) for the indicated periods of time, and the expression levels of c-Abl and PKCδ were determined by immunoblotting with whole cell lysates (β-actin was used as a control for equal loading). The fold change in the protein levels of c-Abl and PKCδ (quantified by densitometry) was determined. **B**, HDMECs were treated with ET-1 (200 n*M*) or vehicle for 2 hours, and cytoplasmic extracts (CE) and nuclear extracts (NE) were prepared. The expression levels of PKCδ were determined by immunoblotting (β-actin was used as a control for equal loading in the analysis of cytoplasmic extracts, and TATA box binding protein [TBP] was used as a control for equal loading in the analysis of nuclear extracts). The fold change in the protein levels of PKCδ was determined. **C**, HDMECs were treated

with scrambled nonsilencing RNA (SCR), small interfering RNA (siRNA) for PKCδ, and siRNA for c-Abl for 48 hours, with or without addition of ET-1 (200 n*M*) for 2 hours. Whole cell lysates were subjected to immunoblotting for c-Abl, PKCδ, and phospho–Fli-1 (β-actin was used as a control for equal loading). The fold change in the protein levels of each molecule (quantified by densitometry) in response to ET-1 as compared to unstimulated controls (set at 1) was determined. Values are the mean ± SEM (n = 3 mice per group). * = $P < 0.05$ versus control cells not treated with ET-1.

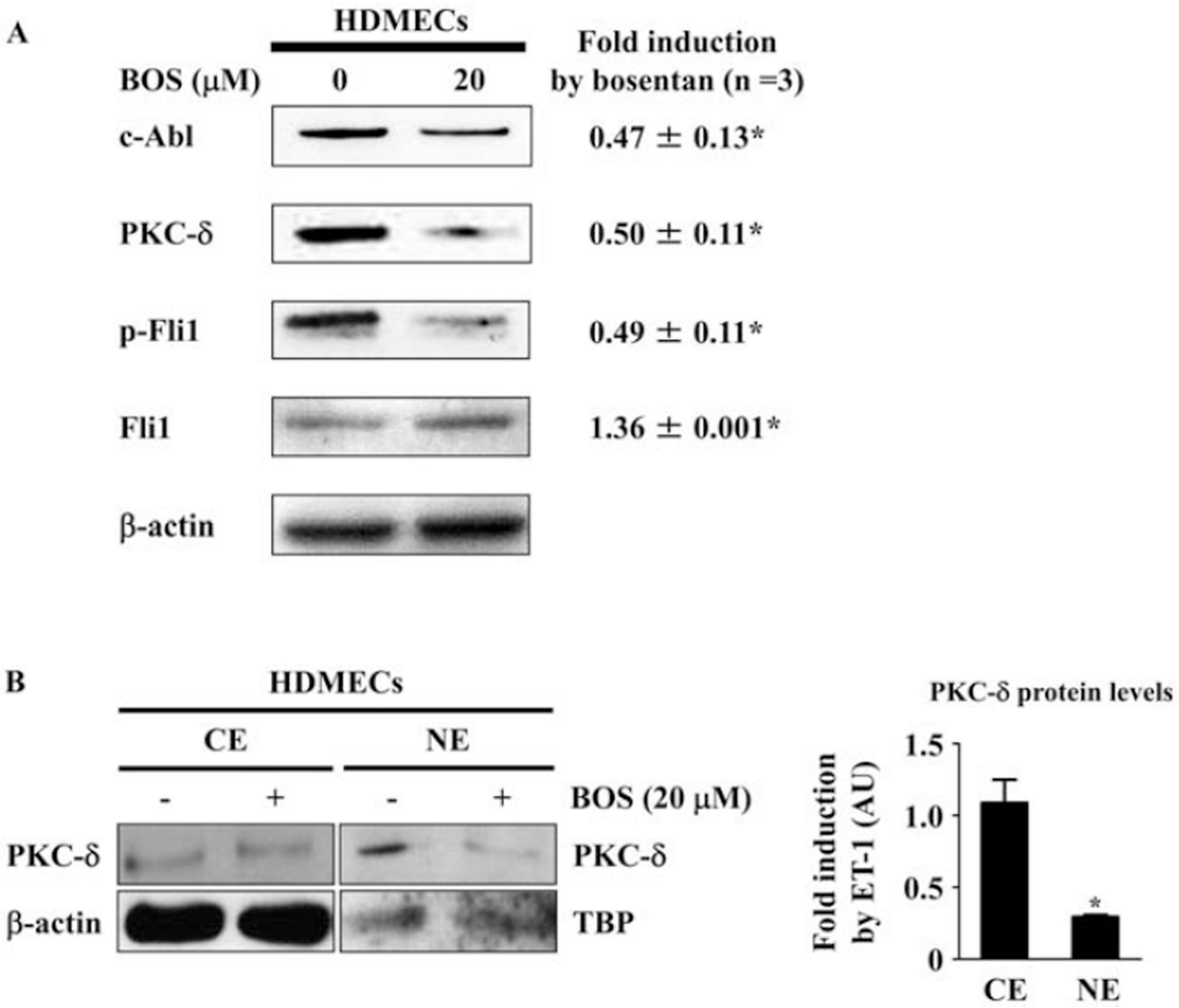

Figure 3.

Impact of bosentan (BOS) on the c-Abl/protein kinase Cδ (PKCδ)/Fli-1 pathway in human dermal microvascular endothelial cells (HDMECs). **A**, HDMECs were treated for 48 hours with bosentan (20μ*M*), and whole cell lysates were subjected to immunoblotting for c-Abl, PKCδ, phospho–Fli-1, and Fli-1 (β-actin was used as a control for equal loading). The fold change in the protein level of each molecule (quantified by densitometry) in response to endothelin 1 (ET-1) as compared to unstimulated controls (set at 1) was determined. **B**, HDMECs were treated with bosentan (20 μ*M*) or vehicle for 48 hours, and cytoplasmic extracts (CE) and nuclear extracts (NE) were prepared (β-actin was used as a control for equal loading in the analysis of cytoplasmic extracts, and TATA box binding protein [TBP] was used as a control for equal loading in the analysis of nuclear extracts). The fold change in the protein level of each molecule in response to ET-1 as compared to unstimulated controls (set at 1) was determined. Values are the mean ± SEM (n = 3 mice per group). * = $P < 0.05$ versus control cells not treated with ET-1.

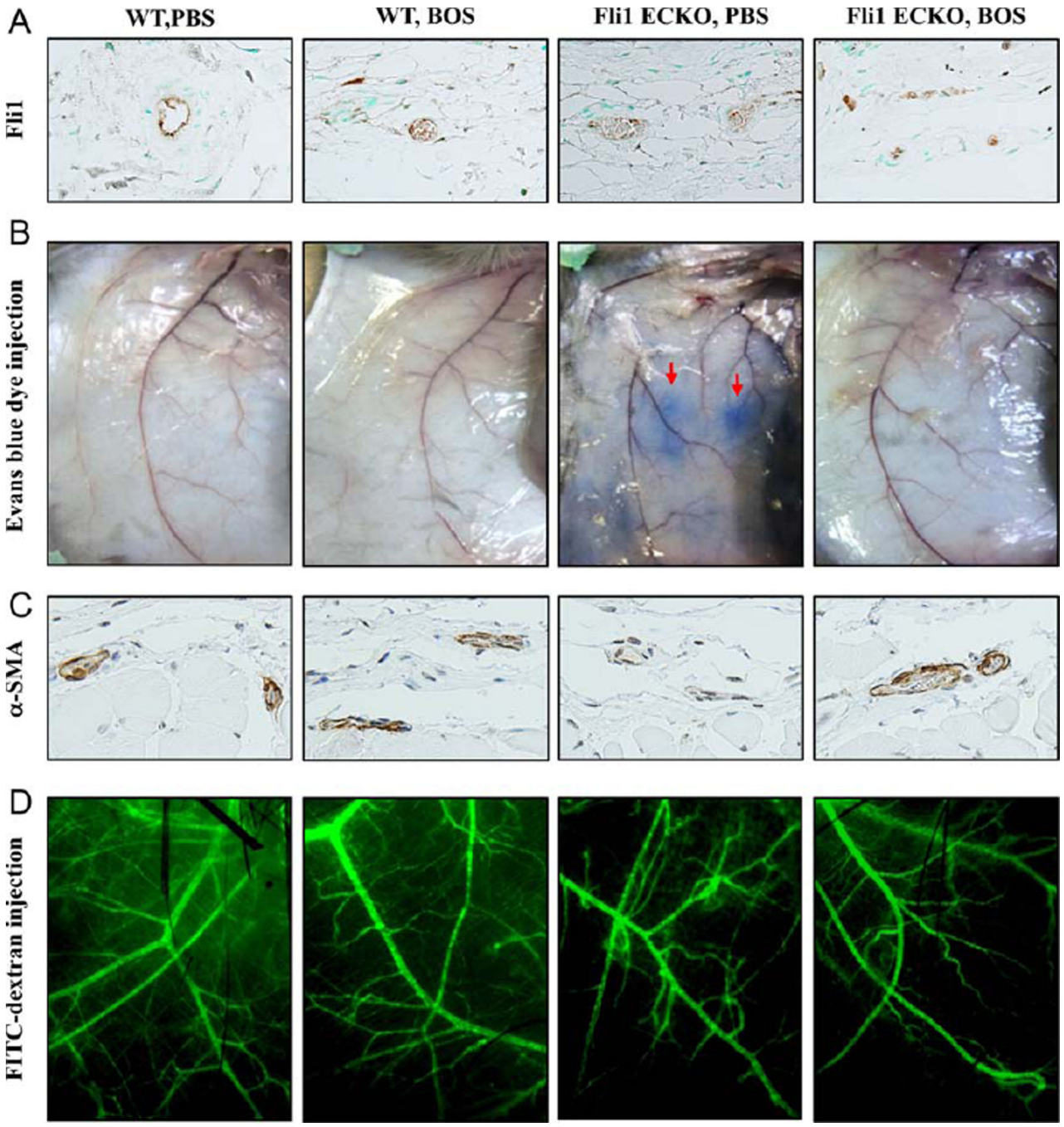

Figure 4.

Effect of bosentan (BOS) on vascular abnormalities in endothelial cell–specific Fli-1–knockout (Fli-1 ECKO) mice. **A**, Wild-type (WT) mice and Fli-1 ECKO mice were injected intraperitoneally with bosentan or phosphate buffered saline (PBS) for 4 weeks. Levels of Fli-1 protein in dermal microvascular endothelial cells were evaluated by immunohistochemistry. **B**, Evans blue dye was injected into the tail vein, and the mice were killed after 30 minutes. The leakage of Evans blue dye (**arrows**) was macroscopically evaluated in the skin. **C**, Levels of α-smooth muscle actin (α-SMA) were determined by

immunohistochemistry. **D**, Mice were injected with fluorescein isothiocyanate (FITC)–conjugated dextran and killed after 5 minutes. The structure of dermal small vessels was examined by fluorescence microscopy. Results are representative of 5 independent experiments.

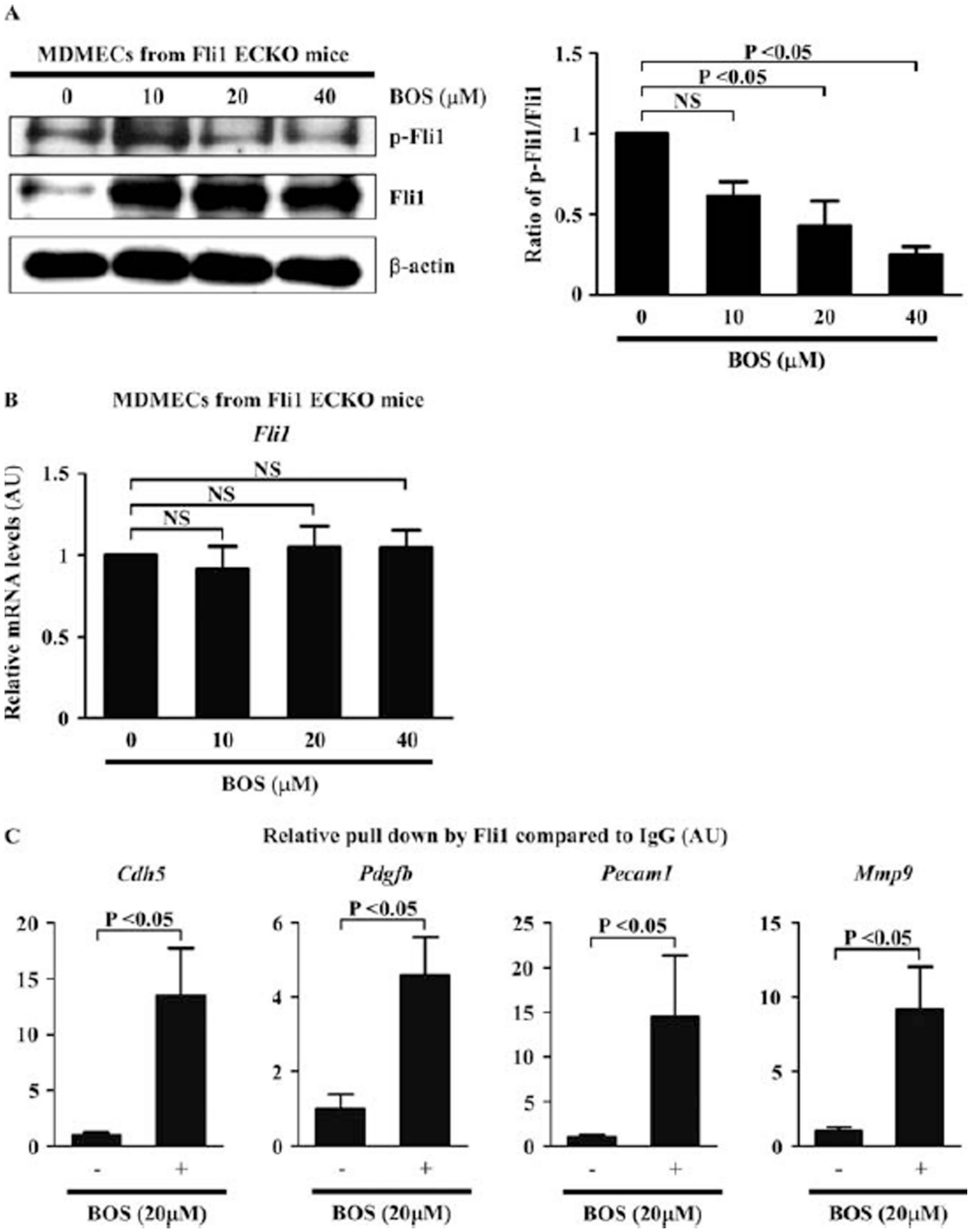

Figure 5.

Effect of bosentan (BOS) on dermal microvascular endothelial cells derived from endothelial cell–specific Fli-1–knockout (Fli-1 ECKO) mice. **A**, Mouse dermal microvascular endothelial cells (MDMECs) isolated from Fli-1 ECKO mice were treated for 48 hours with bosentan at the indicated concentrations, and the expression and phosphorylation levels of Fli-1 were determined by immunoblotting with whole cell lysates (β-actin was used as a control for equal loading). The fold change in the ratio of phospho–Fli-1 to total Fli-1 (quantified by densitometry) was determined. **B**, Levels of mRNA for

Fli-1 after the same treatment as described in **A** were evaluated by quantitative reverse transcription–polymerase chain reaction (qRT-PCR). **C**, MDEMCs were treated with bosentan (20 μ*M*) or vehicle for 48 hours and analyzed by chromatin immunoprecipitation. Binding of Fli-1 to the target gene promoters (*Cdh5*, *Pdgfb*, *Pecam1*, and *Mmp9*) in response to bosentan as compared to unstimulated controls (set at 1) was quantified by qRT-PCR. Values are the mean ± SEM (n = 3 mice per group in **A** and **B** and 4 mice per group in **C**). NS = not significant.